

Incorporating anisotropic electronic structure in crystallographic determination of complex metals: iron and plutonium

K. T. MOORE*[†], D. E. LAUGHLIN[‡], P. SÖDERLIND[§]
and A. J. SCHWARTZ[§]

[†]Lawrence Livermore National Laboratory, Chemistry and
Materials Science, Livermore, CA 94550, USA

[‡]Materials Science and Engineering Department,
Carnegie Mellon University, Pittsburgh, PA 15213, USA

[§]Lawrence Livermore National Laboratory, Physics and
Advanced Technologies, Livermore, CA 94550, USA

(Received 15 November 2006; in final form 22 January 2007)

Anisotropic electronic structure is incorporated in crystallographic determination of the structure of ferromagnetic Fe, δ -Pu and a Pu–3.7 at% Ga alloy. This is achieved by using anisotropic aspects of the inter-atomic bonds as a motif in combination with the high-symmetry cubic lattice. In the case of Fe, it is shown that ferromagnetic ordering reduces the symmetry of the structure from body centred cubic to body centred tetragonal with an associated effect on elasticity. Thus, the ferromagnetic α - and paramagnetic β -phase are separate and unique phases that should both be addressed on the Fe phase diagrams. In the case of Pu, first-principles density-functional theory calculations are used to show that the bond strengths between the 12 nearest neighbours in δ -plutonium vary greatly. Employing the calculated bond strengths as a motif in crystallographic determination yields a structure with the monoclinic space group Cm for δ -Pu rather than face-centred cubic $Fm\bar{3}m$. The reduced space group for δ -Pu illuminates why it is the only metal with a monoclinic ground state, why lattice distortions of the metal are viable and has implications for the behaviour of the material as it ages due to self-irradiation. Results for a Pu–3.7 at% Ga alloy show that the nearest neighbour bond strengths around a Ga atom are more uniform – a result that explains why Ga stabilizes face-centred cubic δ -Pu. This paper illustrates how an expansion of classical crystallography, which accounts for anisotropic electronic and magnetic structure, can explain complex materials in a novel way.

1. Introduction

When determining the space group of a crystal, classical crystallography does not incorporate anisotropic electronic structure within its framework [1]. For some materials, this is unneeded; however, other materials have complicated electronic structures, leading to a myriad of abnormal physical properties. For example, upon heating from room temperature, iron transforms from

*Corresponding author. Email: moore78@llnl.gov

body-centred cubic (bcc) to face-centred cubic (fcc), then back to bcc before it melts. In addition, there is a magnetic–nonmagnetic transition in bcc iron prior to the transformation to fcc, caused by a collective ordering–disordering of the valence electron spins.

Further down the Periodic Table, the actinides possess 5f-electron states at or near the bonding energy level that forms narrow bands. This scenario provides for an inherently unstable situation [2]. Accordingly, the behaviour of the actinide metals is considerably more complex than, for example, aluminium. In the case of iron and plutonium, a more in-depth treatment of the space-group determination of the crystal structure may be in order. With this in mind, this paper illustrates an extended treatment of crystallographic determination of complex materials with anisotropic valence-electron behaviour by incorporating electronic and magnetic structure. For this task, two complex metals have been chosen: one with a ferromagnetic–paramagnetic transition – iron, and the other with highly anisotropic bonding – plutonium. Our goal is to show that this treatment offers a fresh way to interrogate materials with complex electronic structures, yielding a unique way to address outstanding and, in the case of iron, old questions.

1.1. *Iron*

The paramagnetic β -phase in Fe was removed from the phase diagram many years ago and replaced with the same symbol as ferromagnetic α -Fe, due to the belief that the two states – ferromagnetic and paramagnetic – did not constitute different phases of the metal. The β -phase had produced considerable confusion among the metallurgical community, spawning numerous heated arguments. As far as could be determined by X-ray diffraction at the time [3], the structure of ferromagnetic Fe was the same as that of paramagnetic Fe. Since the definition of phase included composition and structure only, no change of phase was deemed to have occurred when Fe lost its ordered magnetism at the Curie temperature.

Differences in magnetic behaviour arise from differences in exchange interactions and magnetocrystalline anisotropy for different materials. Magnetocrystalline anisotropy is linked to the symmetry of the crystal and involves electron spin–orbit interactions and crystal fields [4, 5], and is responsible for generating the directions for the magnetic moments that have minimum energy. The exchange interactions are quantum mechanical phenomena required by the Pauli exclusion principle. For strong exchange, the magnetic moments have a strong coupling to each other and is a cooperative phenomenon. Small exchange interactions yield non-cooperative phenomena. In the case where there is a strong exchange, such as Fe, the valence electrons behave in a highly cooperative and anisotropic manner, which affects the overall symmetry of the structure.

It is not widely known or understood, at present, whether paramagnetic β -Fe and ferromagnetic α -Fe do each indeed constitute a distinct crystal structure, even if the lattice remains bcc in both phases, where $a = b = c$. This will be discussed in detail in this paper.

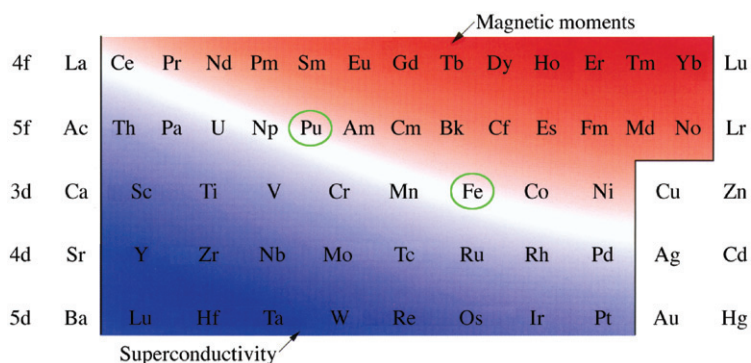


Figure 1. A rearranged periodic table where the five transition metal series 4f, 5f, and 3d to 5d are shown (after [11]). When cooled to the ground state, the metals in the blue area exhibit superconductivity, while the metals in the red area exhibit magnetic moments. The white band running through the middle is where conduction electrons transition from itinerant and pairing to localized and magnetic. Slight changes in temperature, pressure or chemistry will move metals located on the white band to either more bonding or more magnetic behaviour. The two metals examined here, Fe and Pu, are circled in green and show their relation to the magnetic–superconducting transition. For colour, see online.

1.2. Plutonium

Metals that straddle the magnetic–superconducting transition exhibit a fascinating interplay of characteristics, such as itinerant magnetism, heavy fermions, superconductivity and phase instability [6–10]. A rearranged period table is shown in figure 1 containing the five transition metal series: 4f, 5f, and 3d to 5d [11]. At ground state, the metals in the blue area exhibit superconductivity and the metals in the red area exhibit a magnetic moment. The white band is a transition region where metals are on the borderline between localized (magnetic) and itinerant (conductive) valence-electron behaviour. In this transition region, metals such as iron, cerium, neptunium and plutonium are found, each of which can be categorized as a complex metal. Of these metals, plutonium is arguably the most complex with a perplexing electronic structure and, in turn, a myriad of unique properties.

Plutonium exhibits six solid allotropic phases α , β , γ , δ , δ' and ϵ , where the volume of the crystal first expands upon heating then condenses, as shown in figure 2 [12]. The α -phase is simple monoclinic, β is base-centred monoclinic, γ is orthorhombic, δ is fcc, δ' is tetragonal, and finally ϵ is bcc. This is followed by the liquid phase, which not only emanates at a very low temperature for a metal ($\sim 640^\circ\text{C}$), but also is *more* dense than the previous phase, similar to H_2O . Also note from figure 2 that δ and δ' have a negative coefficient of thermal expansion, a quite unusual property for any metal. The oddity of Pu is further illustrated in the pseudo-binary phase diagram of the light actinides in figure 3 [12]. Note how both the melting temperature drops and the number of solid allotropic phases increases along the series when approaching Pu. This reveals that Pu is at the zenith of complex behaviour for the 5f metal series.

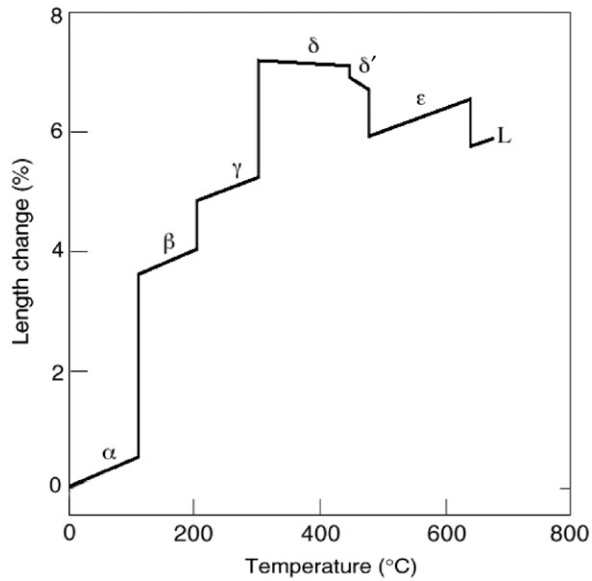


Figure 2. Pu phase diagram showing the large number of solid allotropic phases, the negative coefficient of thermal expansion exhibited by δ and δ' , and the density increase that occurs upon melting.

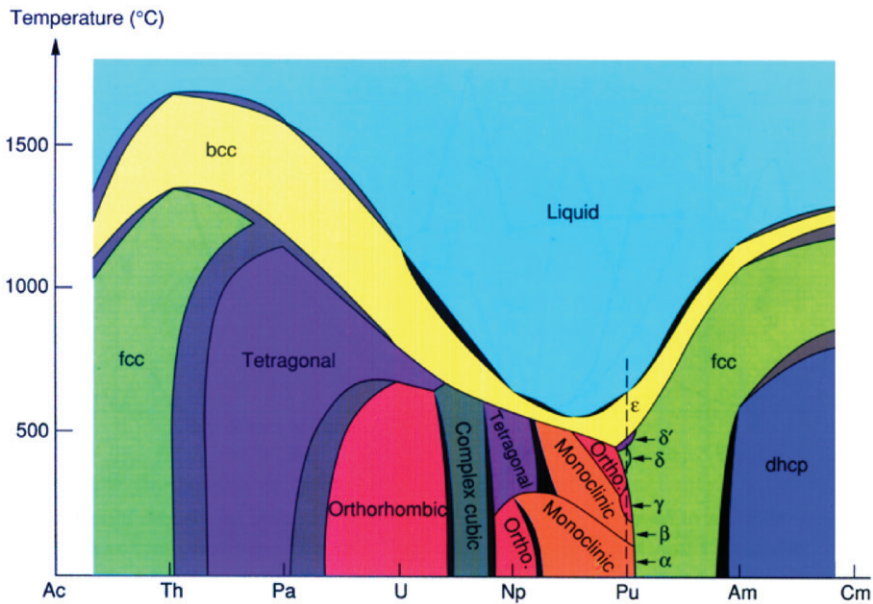


Figure 3. A pseudo-binary phase diagram of the light actinide metals near Pu. Note the increase in the number of solid allotropic phases and the decrease in melting temperature that occur near Pu.

The phonon dispersion curves for δ -plutonium provide yet another intriguing characteristic of the metal. Inelastic X-ray scattering recorded from single-grain regions of δ -plutonium [13], as well as other measurements [14, 15], show that it is the most anisotropic face-centred cubic (fcc) metal known. The shear moduli C_{44} and C' differ by a factor of ~ 7 , which is in strong contrast to the factor of 1.2 found in aluminium [16]. The negative coefficient of thermal expansion, expanded fcc phase unit cell volume, and a huge difference in shear moduli suggest that the bonding strengths between the 12 nearest neighbours of the fcc δ -Pu lattice are not equal. In turn, this means that the total symmetry of the metal may not be fcc, but rather a lower symmetry class [17].

1.3. Aims of this paper

- (1) To illustrate that augmenting classical crystallography to account for anisotropic valence electron behaviour is feasible and can be used to explain unusual behaviour of complex materials in a unique way. To do this, two elements are addressed that reside on the superconducting–magnetic transition in figure 1, i.e. iron and plutonium.
- (2) To show that the paramagnetic β -phase of iron is correctly a phase unto itself with a different symmetry than the paramagnetic α -Fe. Thus, the β -phase should be incorporated into iron phase diagrams. The magnetic moment on each atom of ferromagnetic α -Fe reduces the total symmetry of the structure, in turn altering the macroscopic physical properties observed, such as elastic constants, shear modulus and phase transformations. β -Fe is bcc; α -Fe is tetragonal.
- (3) To systematically progress through crystallographic arguments showing that the high temperature δ -phase in unalloyed Pu belongs to the monoclinic space group Cm rather than the cubic space group $Fm\bar{3}m$. This is achieved using first-principles density-functional theory calculations to obtain the bond-strengths between the 12 nearest neighbours and, in turn, using these bonds as a motif for crystallographic determination. Our results provide new insight into why plutonium is highly anisotropic, why it is the only metal with a monoclinic ground state and why tetragonal, orthorhombic or monoclinic distortions of δ -Pu are likely.
- (4) Results are presented for a metastable δ -phase Pu–3.7 at% Ga alloy, which show that the bond strengths around the Ga atom are more uniform than for a Pu atom surrounded by other Pu atoms. This result illuminates why Ga acts to stabilize the fcc δ -phase over the monoclinic α -phase at room temperature. Results for both pure Pu and Pu–Ga have ramifications for the behaviour of the metal as it ages, accumulating damage via self-irradiation. This will be discussed.

2. Calculation methods

For Pu bond strengths, full-potential linear-muffin-tin orbital (FPLMTO) calculations [18] were employed, since these have been used extensively and successfully for transition [19] and actinide [20] metals. The ‘full potential’ refers to the use of non-spherical contributions to the electron charge density and potential. This is accomplished by expanding these in cubic harmonics inside non-overlapping muffin-tin spheres and in a Fourier series in the interstitial region. We use two energy tails associated with each basis orbital and for the semi-core 6s, 6p, and valence 7s, 7p, 6d, and 5f states, these pairs are different. Spherical harmonic expansions are carried out through $l_{\max}=6$ for the bases, potential and charge density. For the electron exchange and correlation energy functional, the generalized gradient approximation (GGA) is adopted [21]. The nearest-neighbour bond strengths are obtained from total energy calculations of a 27-atom super-cell that uniquely defines all 12 nearest neighbours (NN). By introducing a small (2%) displacement along each of the 12 NN bonds, the force associated with the respective bond is obtained from the corresponding energy shift scaled by the magnitude of the displacement. This is the ‘bond strength’. The super-cell is allowed to spin polarize ferromagnetically, whereas the spin-orbit interaction is omitted to simplify the calculations. It has been shown that spin-orbit interactions are strong in the 5f states of the actinides [22, 23]. However, the spin-orbit splitting that occurs in the 5f states can be mimicked by ferromagnetic ordering [24]. While not strictly correct, because experiments do not confirm ferromagnetism in δ -Pu, this ordering greatly simplifies the complex and time-consuming calculations while still giving an accurate equilibrium volume, bulk modulus and elastic constants [25, 26]. Integration over the irreducible wedge of the Brillouin zone (IBZ, 1/4th of the full zone) is performed using the special k-point method [27] with 20k points in the IBZ for the fcc super-cell. The elastic constants for iron were obtained from the total-energy response of volume-conserving tetragonal (C') and orthorhombic (C_{44}) distortions of up to 1%.

3. Results

To progress our argument that classical crystallography can be augmented to account for anisotropic valence electron behaviour, we will begin with a two-dimensional plane group, then proceed to three-dimensional space groups. Both Fe and Pu will be considered in the progression of this argument, but each will be addressed separately in the discussion section.

We begin in two-dimensions with an array of blocks, as shown in figures 4a and b. A square array of points is first created, which is the *lattice*. Blocks are then incorporated around each lattice point, which is the *motif*. The combination of a lattice and motif in two dimensions results in a two-dimensional structure that has a unique two-dimensional *plane group* of symmetry $4mm$, because there is an axis of 4-fold rotation about each lattice point and there are four mirror planes marked m_1 , m_2 , m_3 , and m_4 . When the upper-left and lower-right corners of each block are filled,

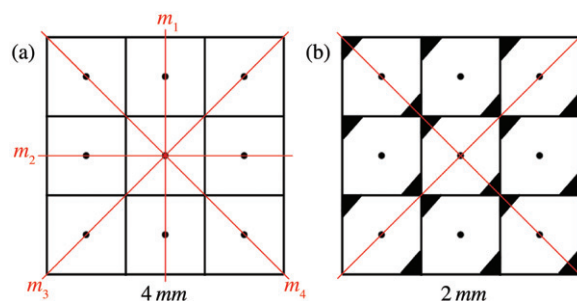


Figure 4. Two periodic arrays illustrating repetition of a lattice (points) and a motif (blocks). (a) Pattern showing a plane group symmetry of $4mm$ and (b) pattern showing a plane group symmetry of $2mm$, reduced only by a change in the motif, not the lattice.

the motif is altered and so is the symmetry of the structure. The plane group symmetry of this structure is reduced to $2mm$ due to the loss of 4-fold symmetry and the elimination of the m_1 and m_2 mirror-plane planes. The salient feature is that the structure in figure 4b retains a square lattice, even though the axis of 4-fold symmetry is lost and the *total* symmetry of the structure is reduced.

Body-centred cubic Fe can be utilized as a three-dimensional real crystal structure to progress this idea further. In this case, the three-dimensional lattice and motif result in a three-dimensional structure that has associated with it a unique three-dimensional *space group*. When Fe is paramagnetic, its structure is bcc with the space group $Im\bar{3}m$. However, when the crystal structure becomes ferromagnetic with aligned moments in the $[001]$ direction, the symmetry is reduced to $I4/mmm'm'\dagger$ as shown in figure 5 [28]. From a geometry standpoint $a = b = c$, but the fact that the spins are aligned along the z -axis lowers the symmetry of the crystal structure. Thus, there do not need to be atomic displacements, with a corresponding change in lattice, to reduce the symmetry of the structure. All cubic lattices must have $a = b = c$, but all structures with $a = b = c$ need not have cubic symmetry!

The same point is relayed by the two-dimensional array of blocks in figure 4 (plane group) and the three-dimensional structure of Fe in figure 5 (space group): The lattice itself may appear to remain high symmetry, but the crystal structure as a whole may be reduced in symmetry due to a change in the symmetry of the motif. This is because the symmetry of any plane or space group is composed of the intersection of the symmetries of a lattice and a motif. In ferromagnetic α -iron, the magnetic moment produced by the outermost valence electrons not only lowers the symmetry from cubic to tetragonal, but also alters the macroscopic properties observed, such as elastic constants, shear modulus and phase transformations.

To address this point, we have used density functional theory to calculate the shear moduli C_{44} and C' for both ferromagnetic (FM) α -Fe and paramagnetic (PM) β -Fe. In addition, the calculations for FM α -Fe were performed with (+SO)

\dagger The symbol m' represents a mirror plane combined with time inversion. For example, see [28].

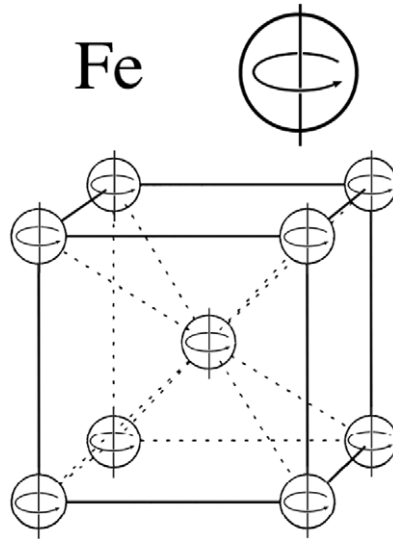


Figure 5. Structure of α -iron. The crystal has a body-centred cubic space group of $\text{Im}\bar{3}m$ when paramagnetic, but is reduced to $I4/m\bar{m}'m'$ when the crystal becomes ferromagnetic with aligned moments in the [001] direction. Note that the atomic positions do not change; rather, the motif is changed by the addition of an ordered magnetic moment, as indicated in the upper-right inset of the figure.

Table 1. Shear moduli C' and C_{44} for both ferromagnetic (FM) α -Fe and paramagnetic (PM) β -Fe calculated by the density-functional theory. For FM α -Fe, the calculations were performed with and without spin-orbit coupling (+SO and -SO, respectively). Finally, experimental values [29] are shown for comparison. The differences between theory (FM) and measurements are close to the expected DFT errors and are partly due to the underestimated lattice constant.

	C'	C_{44}
FM + SO	715	1030
FM - SO	710	1050
PM	-1310	1900
Exp.	525	1219

and without (-SO) spin-orbit coupling. The results are displayed in table 1 and show that, while there is little change between the FM α -Fe calculations with and without spin-orbit coupling, there is a large change between the FM and PM calculations. In fact, the high temperature β -phase comes out unstable in the calculations (negative C'), which is likely because this phase is stabilized by phonon entropies, not included in the zero-temperature calculation. Regardless of the instability, the calculations do indeed show that turning on and off the ferromagnetism in iron does affect the macroscopic properties of the metal substantially. This is observed in experiment, where the elastic anisotropy of ferromagnetically ordered α -Fe is ~ 2.4 at room temperature while paramagnetic β -Fe is ~ 7.1 at 880°C [29].

Table 2. Nearest-neighbour direction in x, y, z coordinates, Miller indices (h, k, l) and bond strength F (mRy/Å) for pure Pu and a Ga atom in a Pu-3.7 at% Ga alloy.

Nearest neighbour (x, y, z)			Miller indices (h, k, l)			Bond strength F (mRy/Å)	
						Pure Pu	Pu-3.7 at% Ga
0.5	0.5	0	1	1	0	4.7	6.3
-0.5	-0.5	0	-1	-1	0	4.5	6.1
0.5	-0.5	0	1	-1	0	3.7	6.3
-0.5	0.5	0	-1	1	0	3.5	6.4
0.5	0	0.5	1	0	1	4.1	7.0
-0.5	0	-0.5	-1	0	-1	3.3	5.6
-0.5	0	0.5	-1	0	1	4.7	4.4
0.5	0	-0.5	1	0	-1	3.9	5.5
0	-0.5	0.5	0	-1	1	3.9	7.3
0	0.5	-0.5	0	1	-1	3.3	5.9
0	0.5	0.5	0	1	1	5.3	6.0
0	-0.5	-0.5	0	-1	-1	3.7	6.0

While a magnetic moment, such as that observed in α -Fe, can reduce symmetry as described above, other aspects of the outermost bonding electrons can also affect the symmetry. In the case of δ -Pu, the phonon dispersion curves have suggested that the bonding strength between the 12 nearest neighbours must not be equal. The question then arises: if an fcc lattice with $a=b=c$ is joined with a motif of anisotropic nearest-neighbour bonds, what is the resultant space group? To address this question, the detailed electronic structure of Pu must be determined, in particular the variation of the nearest-neighbour bond strengths [17]. This was performed by calculating the energy response (ΔE) of a 2% displacement of an atom along each of the 12 nearest-neighbour directions and scaling this with the displacement magnitude ($u=0.049$ Å), as described in section 2. Density-functional theory has proven to be accurate for most metals in the Periodic Table, including Pu [26]; however, its use for calculating bond strength is entirely unique.

The computed bond strengths as calculated by density functional theory are shown in table 2 and figure 6. The nearest neighbour direction (x, y, z) , Miller indices (h, k, l) , change in energy (ΔE) due to a 2% shift of the 0,0,0 atom, and the change in energy normalized by the displacement length ($\Delta E/u$) are shown in table 2. Readily noticeable is that $\Delta E/u$ varies from ~ 3.3 to ~ 5.3 , showing the large degree of variation in bond strength between the 12 nearest neighbours. As shown in figure 6, the 12 nearest neighbours can be separated into six pairs where the bond strengths are close in value: blue (3.3), black (3.5-3.7), red (3.7-3.9), pink (3.9-4.1), green (4.5-4.7) and brown (4.7-5.3). In the (001) plane, the [110] bond is roughly equal to the $[\bar{1}\bar{1}0]$ bond (green), and the $[\bar{1}10]$ bond is roughly equal to the $[1\bar{1}0]$ bond (black). In the {011} planes, we see that $[01\bar{1}] \sim [\bar{1}0\bar{1}]$ (blue), $[0\bar{1}1] \sim [10\bar{1}]$ (red), $[0\bar{1}\bar{1}] \sim [101]$ (pink), and $[011] \sim [\bar{1}01]$ (brown). It is important to note that not only the bond strength, but also the repeatability of groupings dictates the choice of sets. In other words, there is a clear separation between the brown and pink sets and a clear separation between the red and blue sets. It is interesting that the bonds in the (001)

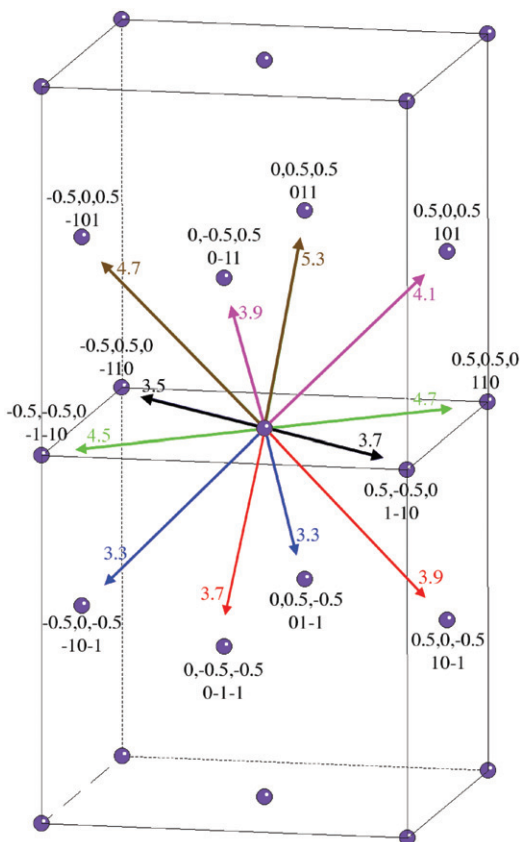


Figure 6. Two stacked fcc unit cells with the central atom showing the 12 nearest neighbours. In the case of plutonium, the 12 bonds with the nearest neighbours widely vary with strength and can be separated into six pairs: blue (3.3), black (3.5–3.7), red (3.7–3.9), pink (3.9–4.1), green (4.5–4.7) and brown (4.7–5.3). When the fcc lattice is combined with the motif of these bond strengths, the resultant space group is monoclinic Cm . For colour, see online.

plane are almost equal directly across the central atom, whereas the bonds in the $\{011\}$ planes are not and have a more complicated arrangement.

When an fcc lattice is joined with the calculated bond strengths as a motif, the resultant structure is c -centred monoclinic with the space group Cm . This low-symmetry space group is due to the fact that, besides translational symmetry, there is no rotational symmetry and only one mirror plane along the (110) plane. The new Bravais lattice for the structure is shown in figure 7, where (a) is the three-dimensional rendering of the c -centred unit cell and (b) is a two-dimensional rendering viewed along the $[001]$ direction. In (b), the fcc lattice is shown by the purple box. The c -centred unit cell is shown by the heavy red box with the green line marking the $[110]$ mirror plane.

This space group has several ramifications. First, it now seems no coincidence that the ground state α -phase of Pu is monoclinic $P2_1/m$ and that here we show

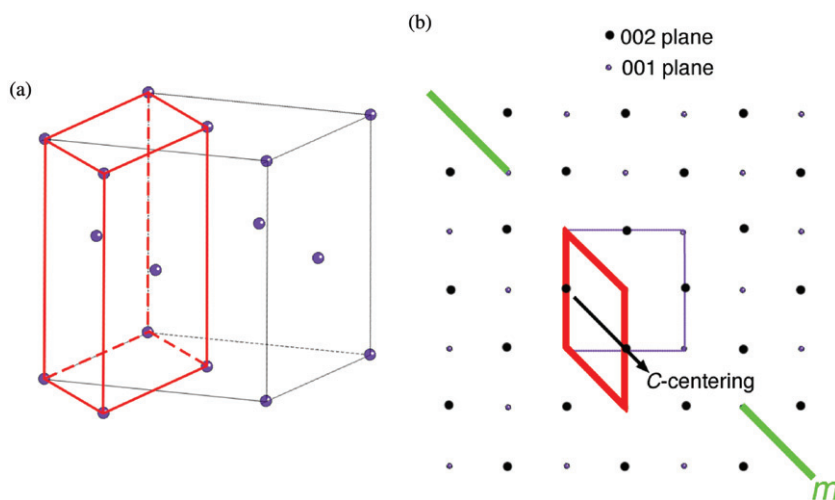


Figure 7. (a) Three-dimensional and (b) two-dimensional representations of the *c*-centred monoclinic Bravais Lattice needed to fully describe δ -Pu.

δ -Pu exhibits a monoclinic space group when the bonding strengths are accounted for as the motif. Also, β -Pu is $C2/m$, where the only difference between the two space groups $C2/m$ and Cm is an axis of two-fold rotation perpendicular to the mirror plane (Of course, in the real structures there is also a slight change of atomic positions). The reduced space group of Cm for δ -Pu yields a viable path for the $\delta \leftrightarrow \alpha'$ phase transformation of Pu and Pu alloys. It has been shown that at low pressures (~ 0.4 GPa), δ transforms first to β' then to α' in Pu-Ce [30] and Pu-Al [31] alloys. Given how close the space groups are between the reduced space group of Cm for δ -Pu and $C2/m$ β -Pu, this intermediate transformation to β is logical.

A second important consequence of these calculations is that the structure is not centrosymmetric; it does not contain the symmetry operation $\bar{1}$. This is apparent in figure 6 from the fact that the bonds in the $\{011\}$ planes are not uniform across the central atom. In the view of classical crystallography, fcc crystals are centrosymmetric; however, the above arguments show that this is not appropriate in describing the symmetry of δ -Pu. The electronic structure (dominated by 5f states) produces bonding in δ -Pu with largely varying strength between the 12 nearest neighbours that does not uniformly exhibit inversion symmetry.

Turning our attention to the metastable δ -phase Pu-Ga alloy, we may now repeat the above calculations with a Ga atom in the central position of our 27-atom super-cell and being subject to the displacement. In this case, we find that the energy response is more uniform than for pure Pu (see table 2). Almost all of the bond strengths are near $F=6$ with the exception of $[010]$ ($F=7.0$), $[0\bar{1}1]$ ($F=7.3$), and $[10\bar{1}]$ ($F=4.4$). Why these bond forces are so high and low in value is not clear; however, the other nine bonds are rather uniform. This uniformity in force implies that the bond strengths surrounding the Ga atom are higher in symmetry, thus supporting a higher-symmetry structure. In other words, these calculations illustrate

why Ga acts to retain the high-symmetry fcc δ -phase at room temperature by making the bond strength about the Ga atom less anisotropic.

4. Discussion

The crystallographic arguments set forth in section 3 illustrate how anisotropy of the chemical bonds can lower the overall symmetry of a given crystal structure. Again, this is due to the fact that the symmetry of a real crystal is given by the intersection of the lattice and motif. For the cases discussed, each atom is the motif and is positioned on a given lattice site. Ferromagnetic Fe has atoms located on a bcc lattice with aligned magnetic moments. δ -Pu is an atom with highly anisotropic bonding set on an fcc lattice. Taking into account these behaviours – ferromagnetism and anisotropic bonding – we find that the total symmetry of the structure is reduced to explain unusual behaviour in complex metals. This idea is unorthodox and creates a number of questions. In the following discussion, we will address the questions set forth in, and those that evolved during, this work.

4.1. Iron

In section 1, the question was raised; ‘is paramagnetic β -Fe a separate phase from ferromagnetic α -Fe?’ The answer is yes. The electron spins align in α -Fe along the z -axis and are coupled to the lattice due to the spin-orbit interaction, creating a moment that changes the motif of the structure. Regardless of whether the bcc arrangement of atoms retains the high symmetry parameters $a=b=c$, the total symmetry is lowered from $Im\bar{3}m$ to $I4/m\bar{m}'m'$ due to the aligned electron spins. The crystal structure of ferromagnetic iron does not have a three-fold axes and has only one four-fold axis.

It has been shown that magnetic point groups can be used to describe the symmetry of crystals which have magnetic moments associated with the atoms [28, 32–37]. In this treatment, phenomena in magnetic materials, such as magnetic domains, domain interactions and magnetostriction, are shown to be more accurately addressed by using the full symmetry aspects of the magnetic state, i.e. the structure with reduced symmetry due to the magnetic ordering. In addition, electronic-structure calculations are required to account for the reduced symmetry due to the ordered magnetic state. Accurate orbital magnetic moments of bcc iron can only be obtained from calculations [38] that consider a lowering of the symmetry, from 48 (cubic) to 8 (tetragonal) operations, due to the preferred orientation of the magnetic spin moments along the [001] easy axis. Cubic symmetry does not support ferromagnetism because the moments always produce a special direction, as shown in figure 5.

Although not cubic, $PrCo_5$ has yielded experimental evidence of symmetry reduction upon magnetic ordering. Shen and Laughlin [39] have shown by convergent beam electron diffraction that the projected point group symmetry along the [0001] direction of $PrCo_5$ is reduced from $6mm$ to 6 on magnetic ordering.

This is consistent with the space group changed from $P6/mmm$ in the paramagnetic state to $P6/mm'm'$ in the ferromagnetic state.

The result of our calculations and arguments is that the β -phase of iron has a different structure than the α -phase and, accordingly, should occupy a separate phase field in the iron phase diagram. The magnetic moment on each atom in α -Fe reduces the total symmetry of the structure from bcc, in turn altering the macroscopic physical properties observed, such as elastic constants, shear modulus and phase transformations.

4.2. Plutonium

The calculations and crystallographic arguments above show that δ -Pu is c -centred monoclinic with the space group Cm when the anisotropic bonds are taken into account. This idea is supported by several of the macroscopic physical properties of the metal. First, δ -Pu is most crystallographically expanded, i.e. lowest density phase of all six allotropes. This is the opposite of almost all other metals in the Periodic Table, where the fcc phase is the most compact and densely packed. This is evidence that the Pu atom cannot be safely assumed to be a hard sphere, as is often done. Second, the coefficient of thermal expansion for δ -Pu is negative. When examining materials with negative thermal expansion, it is obvious that most possess low symmetry structures. Thus, the low density and negative thermal expansion coefficient can be taken as physical affects due to the reduction of symmetry of δ -Pu.

The reduction of symmetry of δ -Pu illustrated above clarifies recent experimental results, such as those from Lawson *et al.* [40, 41], which suggest that a tetragonal distortion occurs in Ga-stabilized δ -Pu. In the work by Lawson *et al.* [40, 41], neutron diffraction revealed that the widths of the peaks were temperature-dependent for $\text{Pu}_{0.98}\text{Ga}_{0.02}$. As the sample was cooled, peak-broadening occurred, increasing with subsequent cooling cycles. This affect disappeared when heated to 650 K. The diffraction peaks were anisotropic, which were modelled by assuming a small tetragonal distortion to the crystal. As the changes in the diffraction peaks were observed at low temperature, it is possible that they are due to the anisotropic response of the δ -Pu matrix to the ingrowth of monoclinic α' -Pu particles, which form during an isothermal martensitic phase transformation at low temperatures [42, 43]. If one introduces precipitates or defects, such as vacancies, interstitials, dislocations and/or He bubbles [44] into an anisotropic medium, the variation in bond strength will cause the lattice to extend more in the soft directions and less in the rigid directions. Thus, tetragonal, orthorhombic or monoclinic distortions in aged Ga-stabilized δ -Pu are logical, because precipitation of second-phase particles or the accumulation of damage will strain the lattice and contract/expand it disproportionately in different directions. Also of note is the small value of C' for δ -Pu [13, 45, 46], which implies a soft response of the system to a volume-conserving tetragonal distortion.

The myriad of crystal structures observed in the actinides, as shown in figure 3, has been addressed by assuming the atoms are ovaloid rather than spherical [47]. The authors suggest this produces the rich polymorphism that is observed in the light-to-middle actinides. We believe that our approach for plutonium and the

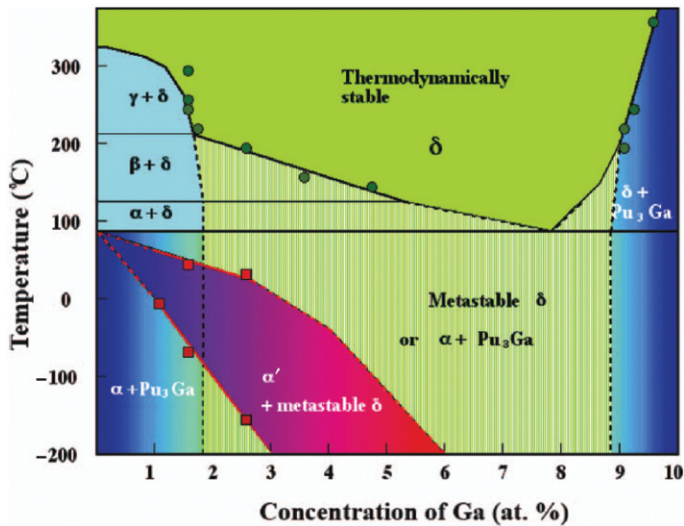


Figure 8. Ga-rich side of the Pu-Ga phase diagram showing the $\delta \rightarrow \alpha'$ isothermal martensitic transformation that occurs at low temperature as a purple-red band [48]. For colour, see online.

discussion by Mettout *et al.* [47] for the actinides are just two different ways of looking at the same issue: anisotropic electronic structure affects the overall symmetry of the crystal structure of actinide metals.

4.3. Pu-Ga alloy

The results for the Pu-Ga alloy shed considerable light on why Ga acts to stabilize, or more accurately retain [12], the fcc structure to room temperature. By reducing the anisotropy of the bonding observed in pure Pu, the structure is allowed to adopt a high-symmetry structure. The amount of Ga will affect how metastable the alloy is by increasing the total number of uniform bonds in the alloy. This is observed in figure 8, which is the Ga-rich side of the Pu-Ga phase diagram, which shows the $\delta \rightarrow \alpha'$ isothermal martensitic transformation as a purple-red band [48]. As the Ga content is increased, the transformation band is suppressed to lower temperatures. Thus, more Ga retards the isothermal martensitic transformation of δ to α' ; conversely, when the Ga content is low, the α' -phase is easily produced either through temperature reduction or an increase in pressure [12]. The high propensity of low-Ga δ -Pu to transform to the α' -phase is again due to the large anisotropy of bonding force between neighbouring atoms of pure Pu.

The extended X-ray absorption fine-structure spectroscopy (EXAFS) results of Cox *et al.* [49] support our calculations for the both pure Pu and the Pu-3.7 at% Ga alloy. In their experiments on Ga-stabilized δ -Pu, it was observed that the local structure of plutonium about the Ga atoms was well defined and similar to a typical fcc metal. However, the local structure of plutonium around Pu atoms was disordered. Our calculations show exactly this: The bonds in pure Pu are highly

anisotropic and, thus, produce a 'poor' fcc structure, whereas the bonds about a Ga atom are less anisotropic and, thus, produce a more typical or 'better' fcc structure, albeit not as good as aluminium.

Extended X-ray absorption fine-structure spectroscopy has also shown that there is a local contraction of the lattice around Ga atoms in Pu–Ga alloys [50]. This is observed in the calculation in table 2, where the bond forces between pure Pu atoms are around $F=4$, whereas the bond forces between Pu and Ga atoms are around $F=6$. This higher bond force means that the strength of the bonds is greater and, accordingly, would cause a contraction of the lattice, as observed by EXAFS.

The above data for pure Pu and Pu–3.7 at% Ga also shed light on the Invar effect observed in plutonium. Pure Pu shows a strong Invar effect where the metal contracts as it is heated [12]. With addition of Ga, the effect reduces and eventually becomes opposite; Pu alloys with moderate amounts of Ga show no thermal expansion, while alloys with greater amounts of Ga have a slight positive thermal expansion. In light of the above calculations, it seems that this effect is the result of the reduction in the bond force anisotropy caused by addition of Ga in the Pu lattice. As more Ga is added, the overall bond anisotropy is reduced and the alloy behaves more like a normal metal, exhibiting a positive thermal expansion.

4.4. *Given anisotropic bonding, can a high-symmetry lattice be retained?*

One may ask: 'As bonding force between the nearest neighbours become more uneven, say moving from Al to Pu, can a high-symmetry lattice be retained?' To address this question, we will consider only cubic crystals and experimental and theoretical results to date.

If one is to imagine a spectrum of elastic isotropy for cubic crystals, Al would reside on one side and plutonium on the other. With this in mind, we performed the same calculations on Al as done for Pu, which is well known to be the most isotropic fcc metal [51, 52]. The results, which are in the same units as the Pu results, lie within 7.55–7.57 for the nearest-neighbour bond strengths. The slight variation in the resulting numbers is numerical noise. This shows that the 12 bonds in Al are all equal in strength and, hence, retain the $m\bar{3}m$ symmetry. When the symmetry of this motif is intersected with the symmetry of the fcc lattice, the $Fm\bar{3}m$ space group is attained. Thus, the fcc structure should be highly stable. This is indeed the case and is illustrated by the Al phase diagram, where the fcc phase is stable from absolute zero to melting at 660°C [53].

In the case of Fe, which falls near the middle of the spectrum of anisotropy and has a strongly aligned magnetic moment in the ferromagnetic structure, there is evidence that the high-symmetry structure is lost. It has been reported that a single crystal and single magnetic domain of Fe has $c/a = 1.3 \times 10^{-5}$ [35]. If correct, this shows the structure has lowered its symmetry from bcc to tetragonal due to the magnetic ordering.

Moving to the far end of the spectrum of anisotropy in fcc crystals, we come to plutonium. The question arises: What is the appearance of δ -Pu symmetry, experimentally, while under normal conditions? Does the lattice remain high-symmetry (i.e. cubic) and only the bonding exhibit the strong anisotropic

behaviour, or does the lattice itself distort to a lower symmetry? This can be examined using high-resolution synchrotron radiation-based X-ray diffraction. While X-ray diffraction does not measure bond energies, it does measure electron charge density. The X-ray scattered intensity for a given reflection is determined by Fourier transform of the charge density [54]. In the case where there is a spherical (isotropic) and non-spherical (anisotropic) part, each can be separated and calculated. The spherical part will be much larger than the non-spherical part, and a rough calculation of the difference in intensity can be obtained by $(1/Z)^2$. In the case of Pu, any additional reflection due to anisotropic distribution of the valence electrons would be approximately 1×10^{-4} weaker than the primary reflections. In reality, additional reflections are probably more on the order of 1×10^{-5} to 1×10^{-6} weaker, and the above simple equation is more accurate for light elements. Thus, we predict that two things could occur: (1) additional weak reflections or highly asymmetric primary reflections would be present due solely to a reduction of symmetry from the valence electrons, and (2) the primary reflections would move a small amount as seen in Fe [35] because the lattice would no longer be $a=b=c$. These effects should be detectable with present synchrotron sources and detectors. Certainly, these experiments should be conducted at the lowest possible temperature to reduce thermal effects[†].

5. Conclusions

The following conclusions can be drawn from this paper:

- (1) When anisotropic electronic structure is incorporated in crystallographic determination of a material, the total symmetry of the structure may be reduced, even though the lattice remains high symmetry. This approach can be used to explain unusual behaviour of complex materials in a new way.
- (2) The β -phase of iron has a different structure than ferromagnetic α -Fe and, thus, is a different phase that should have its own phase field in the iron phase diagram. The magnetic moment on each atom in α -Fe reduces the total symmetry of the structure from bcc to tetragonal, in turn altering the macroscopic physical properties observed, such as elastic constants, shear modulus and phase transformations.
- (3) First-principles density-functional theory calculations are used in a new way to show that the anomalously large anisotropy of δ -plutonium is a consequence of greatly varying bond-strengths between the 12 nearest neighbours. Equipped with these bond strengths, a systematic progression through crystallographic arguments shows that δ -Pu belongs to the

[†]We have attempted detection of extra reflections using electron diffraction in a transmission electron microscope (TEM). However, high thermal diffuse scattering, large amounts of double diffraction due to the high atomic number, and omnipresent surface oxidation have precluded the ability to do this. For these reasons, X-ray diffraction of large, single-grain samples performed at low temperatures will be the appropriate experiment.

monoclinic space group Cm rather than the cubic space group $Fm\bar{3}m$. The reduced-symmetry structure provides new insight into why Pu is the only metal with a monoclinic ground state and why tetragonal, orthorhombic or monoclinic distortions of δ -Pu are likely.

- (4) Results for a Pu–3.7 at% Ga alloy show that the bonding around a Ga atom in Pu is more uniform than for pure Pu. This yields considerable insight into why Ga acts to retain the high-temperature fcc δ -phase to room temperature by alleviating the large anisotropy of bonding.

Acknowledgements

This paper is dedicated to Hub Aaronson, a fiery friend and colleague who we will all miss and who will surely enjoy the stir that our thesis will create. This work was performed under the auspices of the US Department of Energy by the University of California, Lawrence Livermore National Laboratory under contract No. W-7405-Eng-48.

References

- [1] F.D. Bloss, *Crystallography and Crystal Chemistry* (Holt, Rinehart, and Winston, New York, 1971).
- [2] P. Söderlind, O. Eriksson, B. Johansson, *et al.*, *Nature* **374** 524 (1995).
- [3] A. Westgren and G.J. Phragmén, *Iron Steel Inst.* **1** 241 (1922).
- [4] J.M.D. Coey, *J. Appl. Phys.* **49** 1646 (1978).
- [5] C.M. Hurd, *Contemp. Phys.* **23** 469 (1982).
- [6] M.S.S. Brooks, B. Johansson and H.L. Skriver, in *Handbook on the Physics and Chemistry of the Actinides*, edited by A.J. Freeman and G.H. Lander Vol. 1 (North-Holland, Amsterdam, 1984), p. 153.
- [7] L.E. Cox, *Phys. Rev. Lett.* **59** 1240 (1987).
- [8] A.C. Hewson, *The Kondo Problem to Heavy Fermions* (Cambridge University Press, Cambridge, 1993).
- [9] J.L. Sarrao, L.A. Morales, J.D. Thompson, *et al.*, *Nature* **420** 297 (2002).
- [10] K.T. Moore, M.A. Wall, A.J. Schwartz, *et al.*, *Phil. Mag.* **84** 1039 (2004).
- [11] J.L. Smith and E.A. Kmetko, *J. Less Common Metals* **90** 83 (1983).
- [12] S.S. Hecker, *Metall Mater. Trans. A* **35** 2207 (2004).
- [13] J. Wong, M. Krisch, D.L. Farber, *et al.*, *Science* **301** 1080 (2003).
- [14] H.M. Ledbetter and R.L. Moment, *Acta Metall.* **24** 891 (1976).
- [15] R.J. McQueeney, A.C. Lawson, A. Migliori, *et al.*, *Phys. Rev. Lett.* **92** 146401 (2004).
- [16] R. Stedman and G. Nilsson, *Phys. Rev.* **145** 492 (1966).
- [17] K.T. Moore, P. Söderlind, A.J. Schwartz, *et al.*, *Phys. Rev. Lett.* **96** 206402 (2006).
- [18] J.M. Wills, O. Eriksson, M. Alouani, *et al.*, in *Electronic Structure and Physical Properties of Solids*, edited by H. Dreyse (Springer, Berlin, 1998).
- [19] R. Ahuja, P. Söderlind, J. Trygg, *et al.*, *Phys. Rev. B* **50** 14690 (1994).
- [20] P. Söderlind, *Adv. Phys.* **47** 959 (1998).
- [21] J.P. Perdew, J.A. Chevary, S.H. Vosko, *et al.*, *Phys. Rev. B* **46** 6671 (1992).

- [22] K.T. Moore, M.A. Wall, A.J. Schwartz, *et al.*, Phys. Rev. Lett. **90** 196404 (2003).
- [23] G. van der Laan, K.T. Moore, J.G. Tobin, *et al.*, Phys. Rev. Lett. **93** 097401 (2004).
- [24] J.G. Tobin, K.T. Moore, B.W. Chung, *et al.*, Phys. Rev. B **72** 085109 (2005).
- [25] P. Söderlind, A. Landa and B. Sadigh, Phys. Rev. B **66** 205109 (2002).
- [26] P. Söderlind and B. Sadigh, Phys. Rev. Lett. **92** 185702 (2004).
- [27] D.J. Chadi and M.L. Cohen, Phys. Rev. B **8** 5747 (1973).
- [28] D.E. Laughlin, M.A. Willard and M.E. McHenry, in *Phase Transformations and Evolution in Materials*, edited by P. Turchi and A. Gonis (The Minerals, Metals and Materials Society, Warrendale, PA, 2000), p. 121.
- [29] G. Simmons and H. Wang, in *Single Crystal Elastic Constants and Calculated Aggregate Properties: A Handbook* (MIT Press, Cambridge, MA, 1971), pp. 194–197.
- [30] R.O. Elliot, K.A. Gschneidner Jr, US. Patent Office, no. 3,043, 727 (1962).
- [31] E.G. Zukas, in *Proceedings of an International Conference on Solid→Solid Phase Transformations*, edited by H.I. Aaronson (The Metallurgical Society of AIME, Warrendale, PA, 1981), pp. 1333–1337.
- [32] W. Opechowski and R. Guccione, in *Magnetism IIA*, edited by G.T. Rado and H. Suhl (Academic Press, New York, 1965), pp. 105–165.
- [33] A.P. Cracknell, *Magnetism in Crystalline Materials* (Pergamon Press, Oxford, 1975).
- [34] B.K. Vainshtein, *Modern Crystallography I* (Springer, Berlin, 1981).
- [35] S. Shaskolskaya, *Fundamentals of Crystal Physics*, Ch. VIII (Mir Publishers, Moscow, 1982).
- [36] L.A. Shuvalov, *Modern Crystallography IV* (Springer, Berlin, 1988).
- [37] S.J. Joshua, *Symmetry Principles and Magnetic Symmetry in Solid State Physics* (Adam Hilger, Bristol, 1991).
- [38] P. Söderlind, O. Eriksson, B. Johansson, *et al.*, Phys. Rev. B **45** 12911 (1992).
- [39] Y. Shen and D.E. Laughlin, Phil. Mag. Lett. **62** 187 (1990).
- [40] A.C. Lawson, B. Martinez, R.B. Von Dreele, *et al.*, Phil. Mag. B **80** 1869 (2000).
- [41] A.C. Lawson, J.A. Roberts, B. Martinez, *et al.*, Phil. Mag. B **85** 2007 (2005).
- [42] T.G. Zocco, M.F. Stevens, P.H. Adler, *et al.*, Acta Metall. Mater. **38** 2275 (1990).
- [43] K.J.M. Blobaum, C.R. Krenn, M.A. Wall, *et al.*, Acta Mater. **54** 4001 (2006).
- [44] A.J. Schwartz, M.A. Wall, T.G. Zocco, *et al.*, Phil. Mag. **85** 479 (2005).
- [45] X. Dai, S.Y. Savrasov, G. Kotliar, *et al.*, Science **300** 953 (2003).
- [46] G. Robert, A. Pasturel and B. Siberchicot, J. Phys.: Condens. Mater. **15** 8377 (2003).
- [47] B. Mettout, V.P. Dmitriev, M. Ban Jaber, *et al.*, Phys. Rev. B **48** 6908 (1993).
- [48] B. Sadigh and W.G. Wolfer, Phys. Rev. B **72** 205122 (2005).
- [49] L.E. Cox, R. Martinez, J.H. Nickel, *et al.*, Phys. Rev. B **51** 751 (1995).
- [50] Ph. Faure, B. Deslandes, D. Bazin, *et al.*, J. Alloy Comp. **244** 139 (1996).
- [51] H.W. King, J. Mater. Sci. **1** 79 (1966).
- [52] B. Predel and W. Gust, Mater. Sci. Eng. **10** 211 (1972).
- [53] H. Okamoto (Editor), *Desk Handbook: Phase Diagrams for Binary Alloys* (ASM International, Warrendale, PA, 2000), pp. 25–49.
- [54] P. Coppens, *X-ray Charge Densities, & Chemical Bonding* (Oxford University Press, 1997).